Flammability of Polystyrene with Multiple Flame Retardants: Preparation, Characterization, and Response Surface Methodology Optimization

Florencio D. de los Reyes and Magdaleno R. Vasquez

Department of Mining, Metallurgical and Materials Engineering, College of Engineering,

University of the Philippines Diliman, Quezon City 1101, Philippines

Mark Daniel G. de Luna

Department of Chemical Engineering, College of Engineering,

University of the Philippines, Diliman, Quezon City 1101, Philippines

Peerasak Paoprasert*

Department of Chemistry, Faculty of Science and Technology, Thammasat University,

Rangsit Centre, Khlong Nueng, Khlong Luang, Pathum Thani 12120, Thailand

Abstract

The flammability of polystyrene (PS), compounded with silica nanoparticles (SiNPs), 9,10-dihydro-9-oxa-10-phosphaphenantrene-10-oxide (DOPO), and melamine as flame retardants was studied. Surface modification of SiNPs using three silane coupling compounds, 3-aminopropytriethoxy silane (APTES), phenyltriethoxy silane (PHTES), and n-propyltriethoxy silane (PTES), was performed. The flammability of PS, characterized by the limiting oxygen index (LOI), reduced when the flame retardants were added. DOPO exhibited the best flame retardant property, increasing the LOI value of the PS by 42.4 %. A quadratic model for LOI was developed using D-optimal design with the percentage loading of APTES-modified SiNPs, DOPO, and melamine as the independent variables. The response surface methodology was used to explain the synergistic effects of these flame retardants. As the percentage loadings were increased, the observed increase in the LOI value was attributed to both the main effects and interaction effects of the flame retardants.

Keywords: rice husk; silica nanoparticle; polystyrene; flame retardant; surface modification

1. Introduction

The flammability of polymers, especially hydrocarbon polymers, is a significant problem and improvement of flame resistance is needed.

The addition of flame-retardants to highly combustible polymers can reduce fire hazards by increasing the ignition time, decreasing the combustion reaction, and reducing the heat and

flammable gases released (Bar *et al.*, 2015; Salmeia *et al.*, 2015; Fromme *et al.*, 2016; He *et al.*, 2016; Khobragade *et al.*, 2016). Halogen-free compounds, such as phosphorus and nitrogen-containing compounds, are widely used as non-toxic flame retardants (Horacek *et al.*, 1996; Levchik *et al.*, 2006). Nano-fillers can reduce fire hazards by forming a carbonaceous or char layer, which delays fuel release (Beyer, 2002; Joshi *et al.*, 2005; Ou *et al.*, 2009; Kiliaris *et al.*, 2010; Ma *et al.*, 2011; Idumah *et al.*, 2015). A number of silica-based nanomaterials have been studied as potential flame retardants in polymers. These are cheaper, more efficient, and less toxic than the conventional halogen-based compounds, which emit toxic by-products when burnt.

Silica is one of the major components of natural fibers along with cellulose and lignin. It serves as a reinforcement under the cuticles and in the intercellular spaces between cell walls, making the plant structure resistant against collapse. Several plants or plant products contain high levels of silica, including rice husk, bagasse, sugarbeet, and horsetail (Janaun *et al.*, 2016; Kaur *et al.*, 2016; Hariharan *et al.*, 2013; Law *et al.*, 2011). Rice husk contains about 15-20 % silica by weight, depending on factors such as the rice species, the soil conditions, and the climate. Approximately 600 million tons of rice are produced each year worldwide (Le *et al.*, 2013; Adam *et al.*, 2012), yielding about 132 million tons of rice husk. This huge amount of agricultural residue is an environmental problem. Adding value to these wastes is therefore highly desirable.

In recent years, the synthesis of silica from agricultural wastes has been a focus of efforts to address environmental challenges and increase the value of these wastes. Naturally occurring silica in the form of quartz and sands has a crystalline structure and thus a low reactivity that limits its applications (Saleh *et al.*, 2015). In contrast, rice husk-derived silica is amorphous and is attractive in many applications due to its enhanced chemical reactivity, catalytic activity, and mechanical properties. Silica nanoparticles are also high in stability, surface area, and compatibility with other compounds. They have been used in a wide range of applications, as food ingredients, pesticides, fertilizers, additives in polymers, adsorbents, catalysts, and medical additives (Janaun *et al.*, 2016; Hariharan *et al.*, 2013; Wang *et al.*, 2011). Several methods can be used to prepare silica nanoparticles from rice husk, including sol-gel, pyrolysis, and hydrothermal methods. The sol-gel technique is one of the most common methods, producing rice husk derived-sodium silicate precursor, that then hydrolyzes, condenses, and forms silica nanoparticles (Kaur *et al.*, 2016; Le *et al.*, 2013; Wang *et al.*, 2011; Adam *et al.*, 2011; Alshatwi *et al.*, 2015). Metallic impurities and organic matter can be effectively removed by the addition of acid and the use of thermal treatment. The sol-gel method, however, involves several steps and has a long reaction time.

In this study, a method for producing amorphous silica nanoparticles (SiNPs) from rice

husk was developed that used a simple acid treatment and calcination reaction, and did not require the sol-gel step. The flammability of polystyrene (PS) in the presence of SiNPs was studied. PS was chosen as it is widely used as insulation in buildings, and to produce a range of products. The compatibility of silica nano-particles with polystyrene was enhanced by surface modification, using different silane coupling compounds. The PS composites using other flame retardants, including silica nano-particles, DOPO, and melamine, were also studied. Response surface methodology (RSM) was also used to describe the synergistic effects of these flame retardants.

2. Materials and methods

2.1 Materials

Rice husk was obtained from local rice mills in Thailand. Deionized (DI) water was used throughout the experiment. Sulfuric acid, tetrahydrofuran (THF), and toluene were purchased from Carlo Erba Reagents. Melamine, n-propyltriethoxy silane (PTES), phenyltriethoxy silane (PHTES), and 3-aminopropyltriethoxy silane (APTES) were purchased from Sigma-

Aldrich. 9,10-dihydroxy-9-oxa-10-phosphaphe-nanthrene-10-oxide (DOPO) was purchased from Santa Cruz Laboratory (Texas). Polystyrene (PS) was synthesized via classical free radical polymerization using benzoyl peroxide as an initiator. All chemicals were used without purification.

2.2 Synthesis of SiNPs

The rice husk was rinsed with distilled water, sun-dried, and grounded to fine particles. The powdered husk (10 g) was mixed with 30 wt% sulfuric acid (60 mL) in a 250-mL round bottom flask. The mixture was refluxed at 100 °C for 2 h. After cooling to room temperature, the mixture was filtered and washed with DI water. The solid rice husk ash was air-dried and then calcined at 600 °C for 6 h to yield SiNPs as a white powder.

2.3 Surface-modification of silica nanoparticles

The silica nanoparticles were modified using a condensation reaction (Blitz et al., 2014). The stoichiometric amounts of PTES, PHTES, and APTES added were determined using Equation (1) (Hashemi-Nasab et al., 2013).

$$M_x = \frac{S_{SiO_2} \times M_{SiO_2} \times M_x \times available\ OH\ groups \times 10^{18}}{NA} \tag{1}$$

where m_x and M_x represent the weight (g) and molecular weight (g mol^{-1}) of the silane compound (x), S_{SiO_2} is the surface area determined from BET analysis, M_{SiO_2} is the weight of the SiNPs, and NA is Avogadro's number. The stoichiometric amounts of PTES,

PHTES, and APTES from 1 g of SiNPs were 0.43, 0.50, and 0.46 g, respectively.

The amount of silane compounds functionalized on the SiNP surface was determined as the functionalization efficiency:

Functionalization efficiency $= \dfrac{W_2 - W_1}{W_3}$,

where w_1, w_2, and the w_3 are weights of SiNPs, modified SiNPs, and initial silane compounds, respectively.

2.4 Preparation of composites of PS and flame retardants

The preparation method was adapted from a previous study (Bera *et al.*, 2011). Silica nanoparticles and/or flame retardants (20 wt %) were dispersed in tetrahydrofuran. PS was added, and the mixture was stirred at room temperature for 2 h. The mixture was ultrasonicated for an additional 15 min. The mixture was then poured on to an aluminum tray and air-dried for 48 h. It was transferred to a thermal press at 80 °C for 6 h to further remove the bubbles and to control the thickness of the film. The composite film was cut to $130 \times 13 \times 3$ mm^3 and $130 \times 6.5 \times 3$ mm^3 dimension for UL 94 flammability tests and limiting oxygen index (LOI) characterizations, respectively.

2.5 Characterization

The structure and chemical composition of the rice husk-derived silica samples were characterized using XRD (Rigaku PANalytical Xpertpro X-ray diffractometer) and FT-IR (Perkin Elmer Spectrum GX Fourier transform infrared spectrometer). The morphologies and size of the SiNPs were examined using FE-SEM (JEOL JSM-7800F microscope) and DLS (Nano Partica SZ-100 particle size analyzer). Surface area and porosity were characterized using BET and BJH analysis (Quantachrome ASiQwinTM analyzer). The compatibility of the additives was analyzed using an optical microscope. The glass transition (T_g) and thermal degradation (T_D) temperatures of the composites were obtained using DSC (Mettler Toledo DSC1 calorimeter) and TGA (Mettler Toledo TGA/SDTA 851 analyzer), respectively. The flammability of the PS composites was analyzed using limiting oxygen index (LOI), following ASTM D2863. The sample was placed vertically in a test column and then ignited in the presence of nitrogen and oxygen. The minimum concentration of oxygen gas that supports combustion is the LOI value. Horizontal and vertical UL-94 flammability were tested following ASTM D5048 and ASTM D3801, respectively. UL-94 represents the after flame and afterglow time of the sample. The UL-94 results are classified into three categories: (i) V-0: burning stops within 10 sec on a vertical sample, (ii) V-1: burning stops within 20 sec on a vertical sample, and (iii) V-2 burning stops within 30 sec on a vertical specimen. If the sample did not pass the vertical test, the horizontal test was used to measure the linear burning rate. Design-Expert 7.0 software was used to design the experimental runs, using D-optical design, and to analyze the data.

3. Results and discussion

3.1 Synthesis and characterization of SiNPs

SiNPs were synthesized from rice husk using acid treatment and a calcination reaction. The acid treatment removed metal ion impurities and acid-soluble lignocellulosic materials. Finally, calcination of the pre-treated rice husk removed the remaining organic

matters, producing white amorphous SiNPs as a solid powder. The rice husk-derived SiNPs were analyzed using XRD and FT-IR. The XRD pattern confirmed a highly amorphous structure (Figure 1a). The broad signal from 15° to 30° matched previous results on the synthesis of amorphous silica nanoparticles (Alshatwi *et al.*, 2015). There was no indication of crystallinity or other impurities. The FT-IR spectrum showed signals at 3451, 1,100, 802, and 466 cm^{-1}, corresponding to O-H stretching, asymmetric, symmetric, and bending vibrations of SiO_2, respectively (Figure 1b). These peaks were similar to those of the standard silica sample. The XRD and FT-IR results thus confirmed the successful preparation of highly amorphous SiNPs.
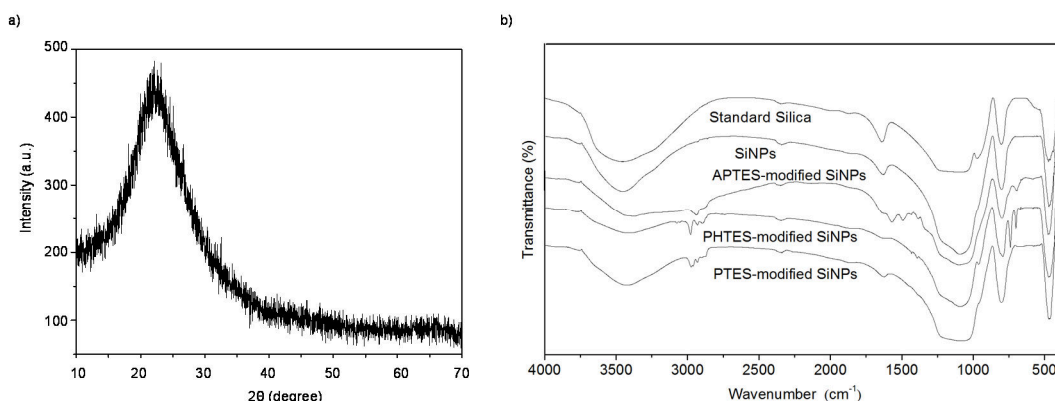

Figure 1 (a) XRD diagram of rice husk-derived SiNPs and (b) FT-IR spectra of standard silica, rice husk-derived SiNPs, APTES-modified SiNPs, PHTES-modified SiNPs, and PTES-modified SiNPs.

The determination of the pore size, porosity, and surface area of nanoparticles is very important as these govern the physical and chemical properties. BET and BJH analysis was used to characterize the surface area and porosity of the SiNPs. The calculated BET surface area, and BJH pore volume, and pore size were 272.7 m^2 g^{-1}, 0.407 mL g^{-1}, and 3.833 nm, respectively, comparable to those reported in previous studies (Le *et al.*, 2013; Wang *et al.*, 2011; Wang *et al.*, 2012).

FE-SEM and TEM were used to analyze the morphology and size of the SiNPs. The FE-SEM and TEM images showed agglo-meration of uniformly spherical particles with particle sizes less than 30 nm (Figure 2 and 3). The particle size distribution of the SiNPs was characterized using DLS, and ranged from 3 nm to 30 nm, with an average diameter of 7.8 nm. This agrees well with the FE-SEM and TEM results.

3.2 Surface-modification of SiNPs

Based on the FT-IR results, SiNPs contained OH groups on the surface. The hydrophilic SiNPs were therefore expected to be incompatible with hydrophobic PS. This aggre-gation was confirmed by the FE-SEM and TEM
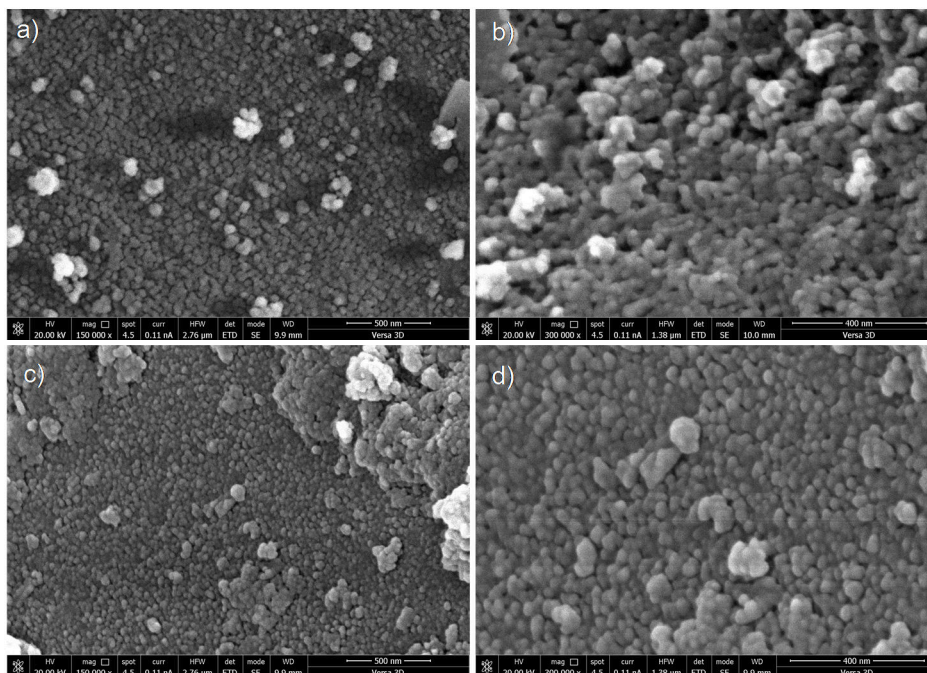
Figure 2 FE-SEM images of SiNPs at (a) 150,000x and (b) 300,000x magnification and APTES-modified SiNPs at (c) 150,000x and (d) 300,000x magnification.
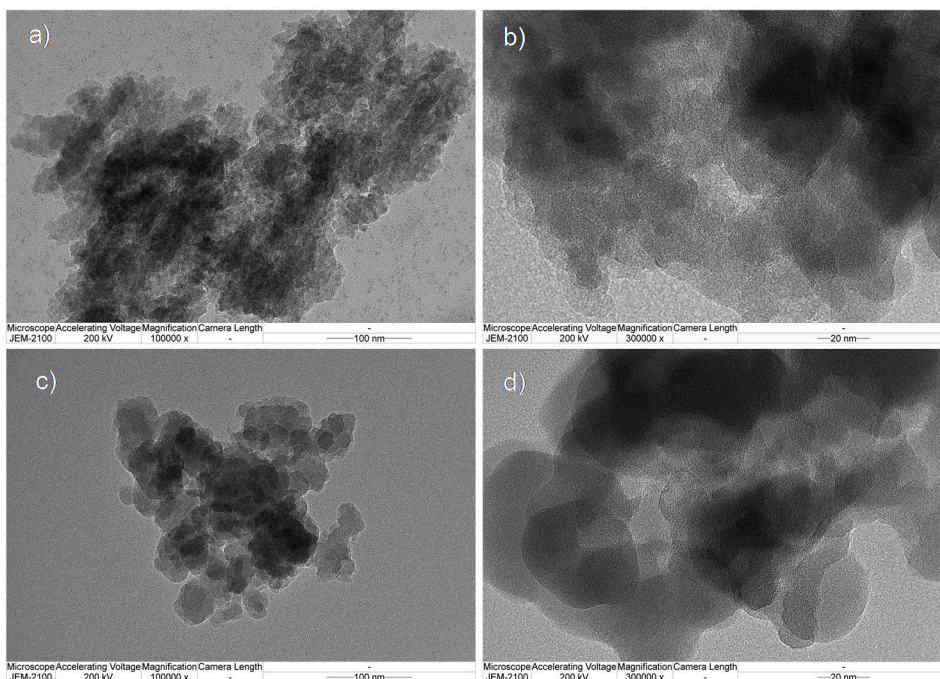

Figure 3 TEM images of SiNPs at (a) 100,000x and (b) 300,000x magnification and APTES-modified SiNPs at (c) 100,000x and (d) 300,000x magnification
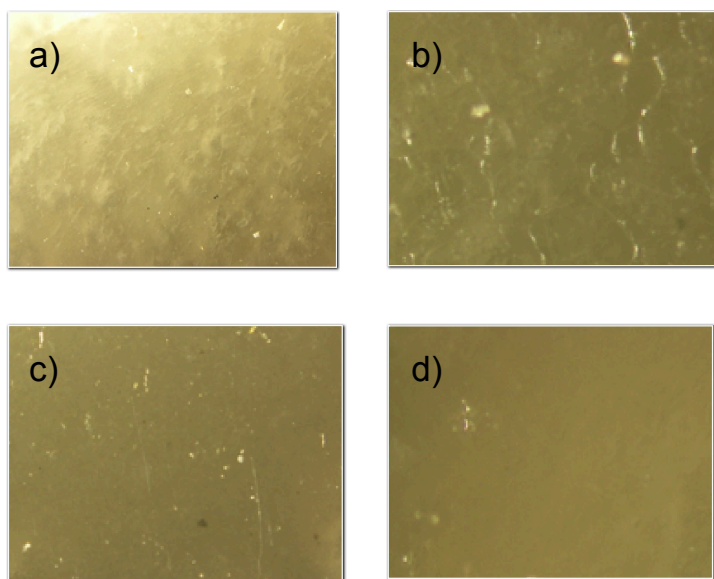
Figure 4 Optical microscopy images of composite films with (a) unmodified SiNPs, (b) APTES-modified SiNPs, (c) PHTES-modified SiNPs, and (d) PTES-modified SiNPs. All images were taken at 400x magnification.

results. The SiNPs were therefore modified using coupling reactions with silane compounds. Silane coupling agents have been reported to increase the hydrophobicity of the silica surface, reducing the aggregation of SiNPs and improving the compatibility of the silica with the polymer matrix (Blitz *et al.*, 2014; Hashemi-Nasab *et al.*, 2013). Three different silane compounds, APTES, PHTES, and PTES, were used. These contain an amine group, a phenyl group, and an alkyl chain, respectively. The stoichiometric amounts of the silane compounds were calculated based on the specific surface area of the synthesized nanoparticles, and using an average silanol content (SiOH) of 4.6 nm^{-1} (Hashemi-Nasab *et al.*, 2013). The functionalization efficiency was calculated using the gravimetric method. The functionalization

efficiencies of APTES, PHTES, and PTES were 25, 17, and 11 %, respectively. APTES was found to be the most efficient silane agent, possibly because the presence of the hydrophilic amine groups led to excellent affinity between the SiNPs and APTES. The functionalization efficiency of ATPES was higher than that previously reported for aminosilanes reacted with silica (Blitz *et al.*, 2014).

The FT-IR spectra of the modified SiNPs showed signals at around 2960 cm^{-1}. These correspond to C-H stretching vibrations, confirming the presence of silane compounds. The broad peak at 3450 cm^{-1} was due to O-H vibrations, indicating the presence of silanol groups in the SiNPs. In addition, the APTES-modified silica showed a characteristic C-N stretching signal at 1500-1600 cm^{-1}. The signal

of an aromatic C-H bending vibration appeared at 700 cm^{-1} for the PHTES-modified silica. The FE-SEM image of the APTES-modified SiNPs showed a greater uniformity in size, shape, and uniformity, compared with the unmodified SiNPs (Figure 4c and 4d), suggesting that the aggregation of the particles was significantly reduced.

3.3 Preparation and characterization PS composites

PS was used to prepare polymer composites with the unmodified and modified SiNPs. Images of the polymer composites were obtained using optical microscopy (Figure 4). The PS composites with unmodified SiNPs had white and cloudy surfaces, reflecting the non-uniformity and presence of aggregates, while the composites prepared from modified SiNPs were clearer, more transparent, and smoother. These results demonstrated that the hydrophilic unmodified SiNPs were not as compatible with PS as the more hydrophobic modified SiNPs.

3.4 Thermal properties of PS composites

The thermal degradation of the PS/SiNPs composites was analyzed using TGA. The onset degradation temperature (T_D) of pure PS was slightly lower than those of the PS with APTES, PHTES, and PTES surface-modified SiNPs additives (Table 1). The presence of SiNPs improved the thermal stability of the polymer films due to the excellent thermal stability of the silica. DSC thermograms of the composite samples were also obtained. The T_g of all the silane-modified SiNPs improved, compared with the pure PS. The increase in T_g

value was due to the strong interactions between the PS and the surface-modified SiNPs (Sun *et al.*, 2004). In the presence of nanoparticles, the free volume was decreased and the polymer chains were harder to move, leading to an increase in T_g values.

Table 1 Degradation temperatures (T_d) and glass transition temperatures (T_g) of polymer composites.

Sample	T_d (°C)	T_g (°C)
PS	403.5	96.22
APTES-modified SiNPs/PS	405.3	98.17
PHTES-modified SiNPs/PS	406.4	98.25
PTES-modified SiNPs/PS	404.5	98.53

3.5 Flammability studies

The use of efficient, cheap, and non-toxic flame retardants (FRs) for highly combustible materials has been explored recently, as alternatives to the conventional halogen-based FRs that produce toxic products upon combustion. In addition to unmodified and modified SiNPs, two further halogen-free compounds, DOPO and melamine, were investigated as FR additives for the preparation of polymer composites with PS. DOPO and melamine are well-known phosphorus- and nitrogen-containing FRs. The flame retarding mechanism of nitrogen-based compounds proceeds via the formation of inert nitrogen gas, whereas phosphorus-containing FRs reduce the amount of free radicals during combustion. This slows down and interrupts the branching and

chain reactions of hydrocarbon oxidation. The flammability of the polymer samples was studied using the test and the UL94 vertical (UL94-V) and horizontal (UL94-H) burning tests. The sample was prepared as a film and placed vertically in a controlled atmosphere. An oxygen/nitrogen mixture was supplied to the bottom of the film, and a candle-like flame was applied to the top to ignite the film. The higher the LOI, the better the flame retarding ability of the material.

Table 2 Limiting oxygen index (LOI) and linear burning rate (UL-94) of PS composites.

Sample	LOI	UL-94 linear burning rate (mm min^{-1})
PS	17.20	157.9
PS/APTES-modified SiNPs	17.90	100.0
PS/PHTES-modified SiNPs	17.20	139.2
PS/PTES-modified SiNPs	17.20	96.43
PS/Melamine	19.20	44.26
PS/DOPO	24.50	V_0

Table 2 shows the LOI values and UL94 test results for the pure PS and polymer composites. APTES, DOPO, and melamine were found to improve the flame retardant properties of PS, whereas the other additives had little effect. Therefore, only APTES-modified SiNPs, DOPO, and melamine were used for the later studies as the multiple flame retardant systems.

3.5 Multiple flame retardant systems and modeling studies

To investigate the use of multiple flame retardants, modeling was also carried out to understand the synergistic effects among the flame retardants. Twenty runs with different amounts of additives were generated using response surface methodology utilizing D-optimal design of experiment, and the LOI values were measured (Table 3). A quadratic model was obtained using the LOI responses. The software generated statistical values for different models and gave the most appropriate model based on the correlation coefficient R-squared and standard deviation (SD) values at the 95 % confidence interval. The model statistics suggested the response surface quadratic model with maximized regression coefficient values of 0.9194, 0.8469, and 0.5411 for R-squared, adjusted R-squared, and predicted R-squared, respectively. The linear and interactive (2FI) models had lower regression coefficient (R^2) values. On the other hand, the cubic model was found to be aliased, implying that there were neither enough unique points nor a correct chosen set of design points.

The model equation for LOI response is given in Equation (2). The coded factors A, B, and C correspond to APTES-modified SiNPs, DOPO, and melamine, respectively.

$$LOI = 21.79 + 0.86A + 1.80B + 1.31C + 0.56AB + 0.65AC + 0.74BC + 0.19A^2 + 0.84B^2 + 0.049C^2 \qquad (2)$$

The analysis of variance (ANOVA) was used to analyze the model equation. A p-value of less than 0.05 implies that the model used is significant. This shows that there can only be a 0.02 % chance that the results obtained using the chosen model was due to nuisance. The Lack of Fit p-Value of 0.2878, which is greater than 0.05, suggests that the model did not detect any Lack of Fit. This insignificance is an indicator that the model fitted with the experimental results, with the actual data points clustered close to the predicted values on the diagonal line, confirming that the chosen model was suitable for predicting the LOI response of the composites (Figure 5a).
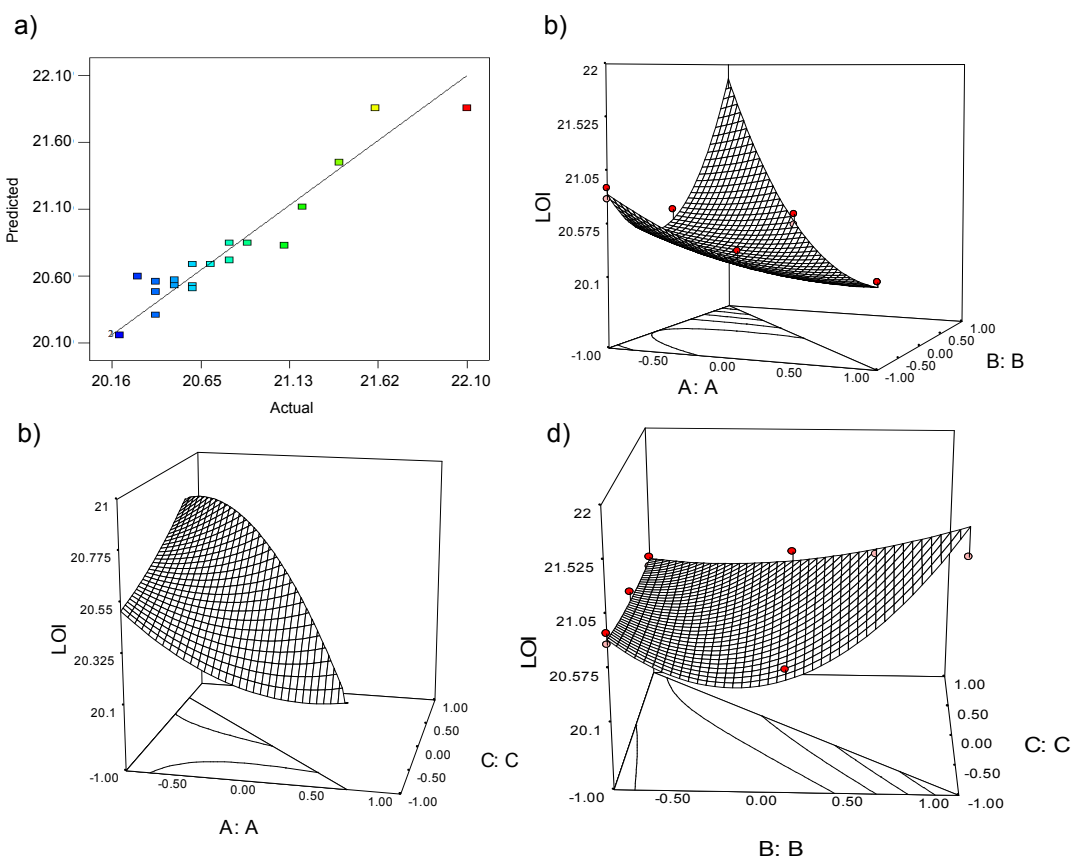

Figure 5 (a) Predicted versus actual values of LOI response and (b) three-dimensional response surface plots of FR loading and LOI for (b) SiNPs and DOPO, (c) DOPO and melamine, and (d) SiNPs and melamine.

The model equation was consistent with the ANOVA statistics on the main effect of the three flame retardant additives on the response. All parameters suggest a positive effect on the response, with DOPO contributing the greatest influence, with a coefficient of 1.80,

among the first-order terms. The positive sign of the coefficients implies that an increase in the amount of these FRs increased the LOI of the composites and therefore improved flame retardance.

The synergistic effects of the three flame retardant additives, APTES-modified SiNPs (A), DOPO (B), and melamine (C), were analyzed using three-dimensional (3D) response surface plots and contour plots generated by the Design-expert 7.0 software (Figure 5b-5d).(Kiliaris, *et al.*, 2010) The interaction of the APTES-modified SiNPs and DOPO is characterized by the difference in their slopes. At any loading of SiNPs, the LOI values increased as the DOPO concentration was increased. Conversely, the LOI value increased as the loading of SiNPs was increased only at high loadings of DOPO. This effect of adding SiNPs on the flammability response of PS was also observed in the interaction plots of the APTES-modified SiNPs and melamine where a significant increase in the LOI was observed as the loading of SiNPs was increased only at high concentrations of melamine. Lastly, the interaction of DOPO and melamine is shown. At low or high percentage loadings of DOPO, the LOI values increased in line with the melamine loading. The same behavior was observed when the DOPO loading was increased. In all cases, the effect of SiNPs as a flame retardant in polystyrene was greatly enhanced by the addition of DOPO or melamine.

A three-dimensional cube plot was used to explore the design points and predict the LOI based on the model used. The edges gave predicted LOI responses between 20.16 and 28.79, corresponding to the levels of the parameter. It was found that the predicted and experimental values were close, with relative errors less than 2 % for two different FR loadings. This confirms the validity of the model for predicting the LOI of PS composites with SiNPs, DOPO, and melamine.

4. Conclusions

In this work, amorphous silica nano-particles were successfully synthesized from local rice husk, using a simple acid treatment and calcination reaction, and without applying the sol-gel method. The rice husk-derived SiNPs had an average diameter of 7.8 nm and surface area of 272.7 m^2 g^{-1}. The SiNPs were highly spherical, with a narrow size distribution between 3 to 30 nm and a pore volume of 0.406 mL g^{-1}. The aggregation of SiNPs was greatly reduced by surface modification using APTES, PHTES, and PTES silane coupling compounds. The compatibility of the surface-modified SiNPs and hydrophobic polystyrene was improved, as aggregation of SiNPs was reduced in the PS matrix. The thermal degradation and glass transition temperature of the PS/SiNPs composites increased due to the good filler-matrix interaction. APTES-SiNPs were found to be the best FR among the three. Flammability studies on PS suggested that DOPO, melamine, and APTES-SiNPs improved the flame retarding ability of the polymer. DOPO exhibited the best flame retarding property, increasing the LOI

value of the PS composite from 17.2 to 24.5 %, classified as V_0 in the UL-94 test. RSM modeling was used to study the synergistic effects of FRs and was found to be in good agreement with the experimental results. This work thus demonstrates that SiNPs from rice husk can be used as an FR. Multi-component systems with different FRs produce synergistic flame retardance properties, maximizing their performances.

5. Acknowledgements

6. References

Adam, F., Andas, J. and Rahman, I.A., 2011, The Synthesis and Characterization of Cobalt-Rice Husk Silica Nanoparticles, Open Colloid Sci. J. 4: 12-18.

Adam, F., Appaturi, J.N. and Iqbal, A., 2012, The utilization of rice husk silica as a catalyst: Review and recent progress, Catalysis Today 190: 2-14.

Alshatwi, A.A., Athinarayanan, J. and Periasamy, V.S., 2015, Biocompatibility assessment of rice husk-derived biogenic silica nanoparticles for biomedical applications, Mater. Sci. Eng. C 47: 8-16.

Bar, M., Alagirusamy, R. and Das, A., 2015, Flame retardant polymer composites, Fibers Polym. 16: 705-717.

Bera, O., Pilić, B., Pavličević, J., Jovičić, M., Holló, B., Szécsényi, K.M. and Špirkova, M., 2011, Preparation and thermal properties of polystyrene/silica nanocomposites, Thermochimica Acta 515: 1-5.

Beyer, G., 2002, Nanocomposites: A new class of flame retardants for polymers, Plast. Addit. Compound. 4: 22-28.

Blitz, J.P., Gun'ko, V.M., Samala, R. and Lawrence, B.A., 2014, Mixed bifunctional surface-modified silicas using tethered aminofunctional silane catalysts, Colloids Surfaces A: Physicochem. Eng. Aspect. 462: 1-8.

Fromme, H., Becher, G., Hilger, B. and Völkel, W., 2016, Brominated flame retardants – Exposure and risk assessment for the general population, Int. J. Hyg. Environ. Health 219: 1-23.

Hariharan, V. and Sivakumar, G., 2013, Studies on synthesized nanosilica obtained from bagasse ash, Int. J. Chem. Tech. Res. 5: 1263-1266.

Hashemi-Nasab, R. and Mirabedini, S.M., 2013, Effect of silica nanoparticles surface reatment on in situ polymerization of styrene-butyl acrylate latex, Prog. Organ. Coat. 76: 1016-1023.

He, C., Zhang, G., Pan, H., Zhang, X., Dang, J. and Chen, C., 2016, Research progress on smoke suppression of halogen free flame retardant polymer materials, Hecheng Shuzhi Ji Suliao/China Synthetic Resin and Plastics 33: 72-77.

Horacek, H. and Grabner, R., 1996, Advantages of flame retardants based on nitrogen compounds, Polym. Degrad. Stabil. 54: 205-215.

Idumah, C.I., Hassan, A. and Affam, A.C., 2015, A review of recent developments in flammability of polymer nanocomposites, Rev. Chem. Eng. 31: 149-177.

Janaun, J., Safie, N.N. and Siambun, N.J. In Synthesis, characterization and catalytic activity of carbon-silica hybrid catalyst from rice straw, AIP Conference Proceedings, 2016.

Joshi, M., Thakare, V. and Pal, S.K., 2005, Polymer clay nanocomposites for coated textile applications: A perspective, Man-Made Text. India 48: 448-455.

Kaur, T., Singh, G.P., Kaur, G., Kaur, S. and Gill, P.K., 2016, Synthesis of biogenic silicon/silica (Si/SiO_2) nanocomposites from rice husks and wheat bran through various microorganisms, Materials Research Express 3.

Khobragade, P.S., Hansora, D.P., Naik, J.B. and

Chatterjee, A., 2016, Flame retarding performance of elastomeric nanocomposites: A review, Polym. Degrad. Stabil. 130: 194-244.

Kiliaris, P. and Papaspyrides, C.D., 2010, Polymer/layered silicate (clay) nanocomposites: An overview of flame retardancy, Prog. Polym. Sci. (Oxford) 35: 902-958.

Law, C. and Exley, C., 2011, New insight into silica deposition in horsetail (Equisetum arvense), BMC Plant Biology 11.

Le, V.H., Thuc, C.N.H. and Thuc, H.H., 2013, Synthesis of silica nanoparticles from Vietnamese rice husk by sol-gel method, Nanoscale Res. Lett. 8: 58.

Levchik, S.V. and Weil, E.D., 2006, A review of recent progress in phosphorus-based flame retardants, J. Fire Sci. 24: 345-364.

Ma, H., Song, P. and Fang, Z., 2011, Flame retarded polymer nanocomposites: Development, trend and future perspective, Sci. China Chem. 54: 302-313.

Ou, Y.X., Zhao, Y. and Li, X.M., 2009, Flame retardant mechanism of polymer/montmorillonite nanocomposites, Gaofenzi Cailiao Kexue Yu Gongcheng/Polym. Materials Science and Engineering 25.

Saleh, N.J., Ibrahim, R.I. and Salman, A.D., 2015, Characterization of nano-silica prepared from local silica sand and its application in cement mortar using optimization technique, Adv. Powder Technol. 26: 1123-1133.

Salmeia, K.A. and Gaan, S., 2015, An overview of some recent advances in DOPO-

derivatives: Chemistry and flame retardant applications, Polym. Degrad. Stabil. 113: 119-134.

Sun, Y., Zhang, Z., Moon, K.S. and Wong, C.P., 2004, Glass transition and relaxation behavior of epoxy nanocomposites, J. Polym. Sci. B: Polym. Phys. 42: 3849-3858.

Wang, W., Martin, J.C., Fan, X., Han, A., Luo, Z. and Sun, L., 2012, Silica Nanoparticles and Frameworks from Rice Husk Biomass, ACS Appl. Mater. Interfaces 4: 977-981.

Wang, W., Martin, J.C., Zhang, N., Ma, C., Han, A. and Sun, L., 2011, Harvesting silica nanoparticles from rice husks, J. Nanopart. Res. 13: 6981-6990.